Observation of an Exceptional Point in a Chaotic Optical Microcavity

Sang-Bum Lee,[1,2] Juhee Yang,[1] Songky Moon,[1] Soo-Young Lee,[1] Jeong-Bo Shim,[3] Sang Wook Kim,[4] Jai-Hyung Lee,[1] and Kyungwon An[1,*]

[1]*School of Physics and Astronomy, Seoul National University, Seoul 151-747, Korea*
[2]*Korea Research Institute of Standard and Science, Daejeon 305-600, Korea*
[3]*Max Planck Institute for the Physics of Complex Systems, Nöthnitzer Strasse 38, Dresden 01187, Germany*
[4]*Department of Physics Education, Pusan National University, Busan 609-735, Korea*

(Received 27 May 2009; published 25 September 2009)

We present spectroscopic observation of an exceptional point or the transition point between mode crossing and avoided mode crossing of neighboring quasieigenmodes in a chaotic optical microcavity of a large size parameter. The transition to the avoided mode crossing was impeded until the degree of deformation exceeded a threshold deformation owing to the system's openness also enhanced by the shape deformation. As a result, a singular topology was observed around the exceptional point on the eigenfrequency surfaces, resulting in fundamental inconsistency in mode labeling.

DOI: 10.1103/PhysRevLett.103.134101 PACS numbers: 05.45.Mt, 42.55.Sa, 42.65.Sf

Dielectric optical microcavities are widely used in various optoelectronics applications such as add or drop filters, low-threshold microlasers [1], single-molecule sensors [2], tunable optical frequency combs [3], and optomechanical oscillators [4] owing to the high-quality factor Q of supported modes. In addition, asymmetric optical microcavities have drawn much attention because they exhibit directional output emission of high-Q modes. They can also serve as a useful platform for investigating the correspondence between quasieigenstates and associated chaotic classical dynamics in mesoscopic systems due to the well-known one-to-one correspondence between the Schrödinger equation and the Maxwell equation in billiard problems [5]. Level dynamics of interacting modes have also been studied for tailoring output directionality and quality factors of associated modes [6,7].

One of the key issues related to the level dynamics is the exceptional point (EP), a point in the parameter space of a non-Hermitian Hamiltonian where the eigenstates of this Hamiltonian coalesce [8–10]. Consequently, it has peculiar properties such as eigenstate exchange, singular topology, and a nontrivial geometric phase under cyclic parameter variation around it. EPs have been observed in various systems such as acoustic systems [11], atoms in optical lattices [12], and complex atoms in laser fields [13]. In coupled microwave cavities, the EP was studied in terms of resonance mode distributions [14,15]. Existence of an EP has been predicted for mesoscopic systems such as a Rydberg atom in a strong magnetic field [16] and in a stadium-shape microcavity [17], where classical chaos is also important. Yet observation of EPs in these classically chaotic systems has not been reported.

In a recent work of Ref. [18] in a chaotic optical microcavity (COM), depending on the degree of cavity-shape asymmetry we observed either mode crossing (MC) or avoided mode crossing (AMC) when a system parameter was scanned. However, we could not observe an EP, where the transition between MC and AMC occurs in a two-dimensional parameter space. We could not tell whether two modes were crossing each other or if they were avoiding each other with a gap smaller than our spectral resolution. Similar problems were also found with indistinguishable static envelopes of crossing and avoided crossing modes in a high-Q toroidal microcavity [19].

In this Letter, we report the first observation of an EP in a high-Q asymmetric microcavity or COM. Our experiment, done in a single COM and not in coupled cavities as before [14,15], was made possible by introducing an internal parameter, a quasicontinuous variable in a semiclassical regime of large size parameter, and is based on the fact that two modes undergoing an AMC exhibit fundamentally different output coupling signatures from those of MC modes. Moreover, we elucidate the resulting singular topology in the eigenenergy surfaces around the EP as an inherent source of impossibility of consistent mode labeling in open mesoscopic systems.

Our COM is a two-dimensional microcavity formed by a liquid jet of ethanol (refractive index $m = 1.361$ at 610 nm) doped with rhodamine dye molecules and ejected from a deformed orifice. The cavity boundary is approximately given by $r(\phi) \simeq a(1 + \eta \cos 2\phi + \epsilon\eta^2 \cos 4\phi)$ in the polar coordinates with $a \simeq 14.9 \pm 0.1$ μm and $\epsilon = 0.42 \pm 0.05$ [20]. The details of our liquid-jet setup are described in Ref. [21]. In short, the deformation parameter η can be continuously varied from 0% to 26% by changing the ejection pressure of the jet through the orifice. The size parameter, defined as $2\pi ma/\lambda$ with λ the wavelength, is about 190 for $\lambda = 660$ nm.

The COM was pumped by a cw argon-ion laser from the side. Cavity-modified fluorescence (CMF) and lasing light from the COM were measured with a grating spectrometer by the scheme described in Ref. [22]. The polarization

direction for both pumping and detection was parallel to the COM column [18,22,23]. Five different mode sequences recurring with an interval or a free spectral range of about 2.3 THz were observed. Mode label l is assigned to each mode sequence by the scheme explained in Ref. [18] and the recurring modes in a mode sequence are indexed by mode number n.

In Fig. 1, we observe $l = 2$ and $l = 4$ modes undergoing AMCs as a function of η at $n = 179$, 180, 181, and 182, respectively, indicating that the separation of two modes can be adjusted continuously by changing η for a fixed n. We also observe AMCs as we move horizontally for a fixed η from one free spectral range to another. This is equivalent to scanning the mode number n, a discrete internal parameter. The relative frequency between $l = 2$ and $l = 4$ modes is changed by 0.083 THz or 3.6% (when they are well apart) of their FSRs when n is shifted by 1. From the locations of AMCs, $(n, \eta) = (179, 0.162)$, (180, 0.167), (181, 0.172), and (182, 0.176), we also find that the same 0.083 THz induced by n shift can be continuously scanned by changing η by about 0.005. Therefore, by coarse scanning of n shift for a fixed η, followed by a fine adjustment of η within 0.005, we can bring any two modes together, far beyond our spectrometer resolution ($\sim$50 GHz). An exact definition of the internal parameter n is given below when we discuss Fig. 4.

It was shown in Ref. [18] that the mode-mode interaction in a COM can be described by a 2×2 non-Hermitian symmetric Hamiltonian. Its diagonal elements, given by $E_j(n, \eta) = \nu_j(n, \eta) - i\gamma_j(\eta)$ $(j = a, b)$ (with the Planck constant $h = 1$), are the eigenvalues of quasieigenmodes when they are far apart, i.e., effectively uncoupled. The imaginary part corresponds to the decay rate of the mode. The symmetric off-diagonal element, denoted by $C(\eta)$, is the mode-mode coupling constant induced by the cavity-shape asymmetry while its dependence on the internal parameter n is negligible in the small spectral range of interest.

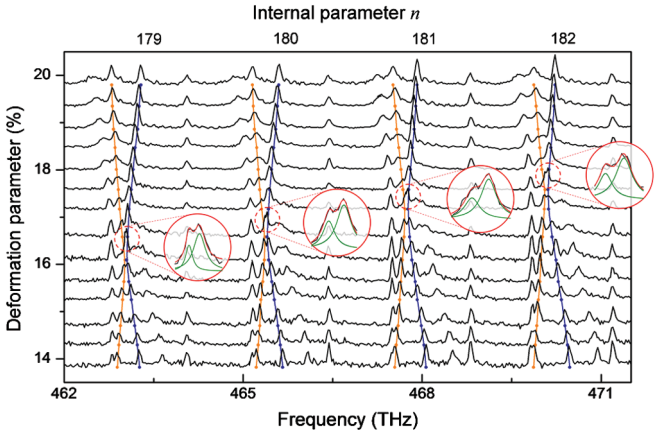

FIG. 1 (color). Eigenfrequencies of $l = 2$ (in orange) and $l = 4$ (in blue) modes as a function of the deformation η and the internal parameter n. The magnified view shows the high resolution spectra taken with a spectrometer of 0.05 nm resolution. Green curves are Lorentzian fits.

The uncoupled quasieigenmodes of different radial mode order have different FSRs. Thus, by shifting the internal parameter n for a fixed η followed by a fine adjustment of η as explained above, we can bring any two uncoupled modes together and make the mode-mode coupling come into play. In this case, the system has new eigenvalues $E_\pm$ given by $E_\pm = (E_a + E_b)/2 \pm \sqrt{(E_a - E_b)^2/4 + C^2}$. When $\nu_a = \nu_b (= \nu_0)$, the new eigenvalues are given by $E_\pm = \nu_0 \pm (C^2 - \gamma_-^2)^{1/2} - i\gamma_+$ with $\gamma_\pm = |\gamma_a \pm \gamma_b|/2$. When $C < \gamma_-$, a splitting occurs in the imaginary part of energy, corresponding to a MC in the real part as we vary n. When $C > \gamma_-$, an AMC, a splitting in the real part, would occur as n is varied. This splitting is analogous to the mode splitting in coupled cavities [14]. However, in our COM, the internal coupling C is induced by the cavity-shape asymmetry, related to chaotic ray transport between phase-space regions associated with the involved quasieigenmodes [18].

It should be noted that $l = 2$ and $l = 4$ modes in Fig. 1 correspond to the new quasieigenvalues $E_\pm$, the result of AMC between uncoupled $j = a, b$ quasieigenmodes. We have systematically measured the sizes of AMC between $l = 2$ and $l = 4$ modes for various cavity deformation ranging from 0.14 to 0.23 as shown in Fig. 2(a). We can also obtain the decay rates or the half linewidths of the uncoupled states in the spectral region where AMC or MC occurs as shown in Fig. 2(b). In fact, we have identified from the spectrum evolution that these uncoupled states have evolved from whispering gallery modes (WGMs) with radial mode order $l_0 = 1$ and 4 in a circular cavity as η is gradually increased [18]. Thus we can label these uncoupled states $j = a, b$ above by the same $l_0 = 1$ and 4 as those of the original WGMs.

It is interesting to note that the observed $\Delta\nu_{14}$s appear to be well fit by a straight line with a η-axis offset, indicating that a threshold deformation for the splitting exists. In other words, the transition from MC to AMC is suppressed up to a threshold deformation due to the openness which is also enhanced by the system's nonintegrability. This feature is quite interesting since the nonintegrability in an open chaotic billiard induces both coupling and openness (the latter summed up by decay rates) to grow. In our example of $l_0 = 1$ and 4, the coupling (initially zero) catches up the decay rates (initially finite) as η grows. Contrarily, in a closed system, an AMC would occur as long as $\eta > 0$, however small it is.

From the η-axis offset of a linear fit in Fig. 2(a), one may expect that the two modes $l_0 = 1$ and 4 would undergo a transition from AMC to MC, or vice versa, at $\eta \sim 0.15$. However, the linewidth of these modes become much narrower ($<$3 GHz) than our spectral resolution once η is decreased below 0.16, and thus we cannot determine the actual value of threshold deformation by simply noting the disappearance of the splitting between the two modes.

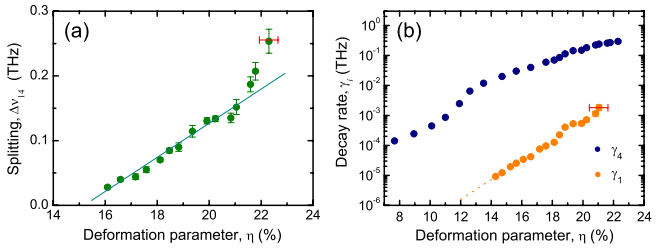

FIG. 2 (color online). (a) Magnitude $\Delta\nu_{14}$ of AMC between two uncoupled states, $l_0 = 1$ and $l_0 = 4$ modes, as a function of η. (b) Decay rates γ_1 and γ_4 of $l_0 = 1, 4$ uncoupled states. The dotted line for γ_1 is an extrapolation beyond spectral visibility.

One can solve this rather inherent problem by realizing that two modes undergoing a MC tend to maintain their original linewidths whereas two modes undergoing an AMC share a common linewidth given by the average (γ_+) of the original linewidths. This fundamental difference is then translated to substantially different output coupling efficiencies for those two cases, as seen below. Here the output coupling efficiency is a measure of relative mode strength seen in the CMF spectrum. According to the cavity quantum electrodynamics [24], the same amount of fluorescence is directed to each cavity mode. However, since the light in a mode (say, the jth mode) is also absorbed by the cavity medium before it decays to the outside, the relative mode strength is then given by the ratio $\epsilon_j = \gamma_j/(\gamma_j + \gamma_{\text{abs}})$, the output coupling efficiency, with γ_{abs} the absorption rate of the medium [25].

For $l_0 = 1$ and 4 modes, we have $(\gamma_1, \gamma_4, \gamma_{\text{abs}}) \sim (2 \times 10^{-6}, 4 \times 10^{-3}, 2 \times 10^{-5})$ THz and thus $\gamma_1 \ll \gamma_{\text{abs}} \ll \gamma_4$ in the spectral region where the transition is expected; therefore, $\epsilon_1 \sim \gamma_1/\gamma_{\text{abs}} \ll 1$ and $\epsilon_4 \sim 1$. This indicates that the $l_0 = 1$ mode is hardly visible while the $l_0 = 4$ mode has almost maximum visibility in the spectrum when these two modes are well separated. This behavior can be seen in Figs. 3(a)–3(c), where $l_0 = 1$ modes are not visible in the CMF spectra, whereas they become prominent when the pump power is increased beyond its lasing threshold as seen in Fig. 3(d).

When an AMC occurs ($C > \gamma_- \sim \gamma_4/2$), the two modes form a doublet with each having the same decay rate of $\gamma_+ \sim \gamma_4/2$. The output coupling efficiency of each is then given by $\gamma_+/(\gamma_+ + \gamma_{\text{abs}}) \equiv \epsilon_+ \sim 1$. When the two modes barely undergo an AMC, they appear to be overlapped into a single peak in the spectrum with its output coupling efficiency given by $\epsilon_{\text{AMC}} = 2\epsilon_+ \sim 2$. This effect is clearly observed in Fig. 3(a), where the peak at 664.5 nm is two times larger than the other $l_0 = 4$ modes, indicating that an AMC takes place there between $l_0 = 1$ and 4 modes.

When the two modes undergo a crossing ($C \leq \gamma_-$), on the other hand, the decay rate of each mode is modified from its original value as $\gamma_1' = \gamma_+ - (\gamma_-^2 - C^2)^{1/2}$ and $\gamma_4' = \gamma_+ + (\gamma_-^2 - C^2)^{1/2}$. The resulting output coupling efficiency when the two modes are overlapped is then given by $\epsilon_{\text{MC}} = \gamma_1'/(\gamma_1' + \gamma_{\text{abs}}) + \gamma_4'/(\gamma_4' + \gamma_{\text{abs}}) \leq$

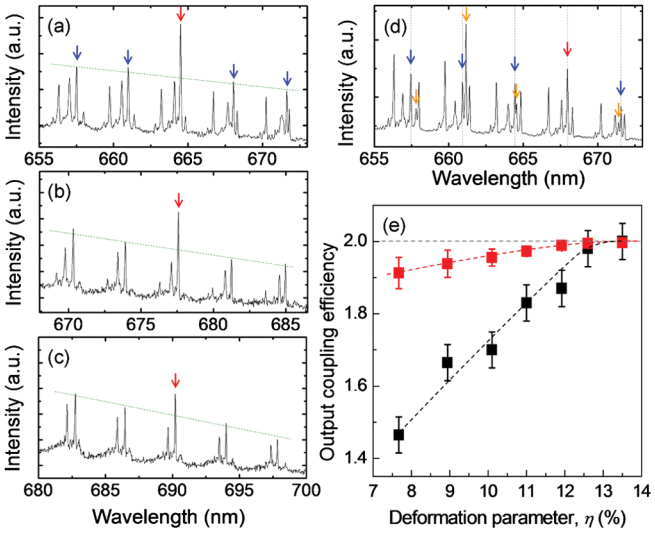

FIG. 3 (color). CMF spectra for the case of (a) $\eta = 0.125$, (b) $\eta = 0.102$, and (c) $\eta = 0.078$. Orange and blue arrows indicate $l_0 = 1$ and $l_0 = 4$ modes, respectively. The output coupling efficiency of $l_0 = 1$ modes is too small for these modes to be observed in (a)–(c). Red arrows indicate where $l_0 = 1$ and 4 modes appear to be overlapped. Deformation η was fine-tuned within 0.005 to maximize the peak. (d) Pump power is increased above a lasing threshold for $l_0 = 1$ mode at 661 nm with $\eta = 0.120$. $l_0 = 1$ modes are clearly seen. (e) Observed output coupling efficiency (black squares) compared to $2\epsilon_+$ (red squares). Slight reduction in $2\epsilon_+$ itself is mostly due to the decrease of decay rates of the involved modes. The black dotted line is a spline fit for visual guidance.

ϵ_{AMC}, where the equality holds when $C = \gamma_-$ or at the transition point. Particularly, if $C \ll \gamma_-$, we have $\gamma_1' \sim \gamma_1$ and $\gamma_4' \sim \gamma_4$, and the corresponding output coupling efficiency is approximately given by $\epsilon_{\text{MC}} \sim 1$. Therefore, the transition from AMC to MC is signaled by a substantial reduction of the output coupling efficiency from $2\epsilon_+$, as seen in Figs. 3(b) and 3(c), when two modes appear to be overlapped.

We examined the output coupling efficiency (black squares) when $l_0 = 1$ and 4 modes appear to be overlapped. We observed that this coupling efficiency starts to deviate noticeably from $2\epsilon_+$ (red squares) as the deformation parameter is reduced below 0.125 as shown in Fig. 3(e). From this observation, we conclude that the two modes undergo a transition from AMC to MC, or vice versa, at $\eta_0 = 0.125 \pm 0.005$.

A parameter-space point at which the transition from MC to AMC takes place or $E_\pm$ states coalesce is the EP, a topological singular point. The singular nature of the EP is revealed when we examine the eigenfrequency surfaces of $l = 2$ and 4 modes in a n-η parameter space. The eigenfrequency surfaces $E_\pm(n, \eta)$ are constructed in the following way. We first define reference frequencies as the resonance frequencies of $l_0 = 3$ WGM in a circular cavity whose round-trip length is the same as that of the COM under investigation, as shown in Fig. 4(a). The spectrum is

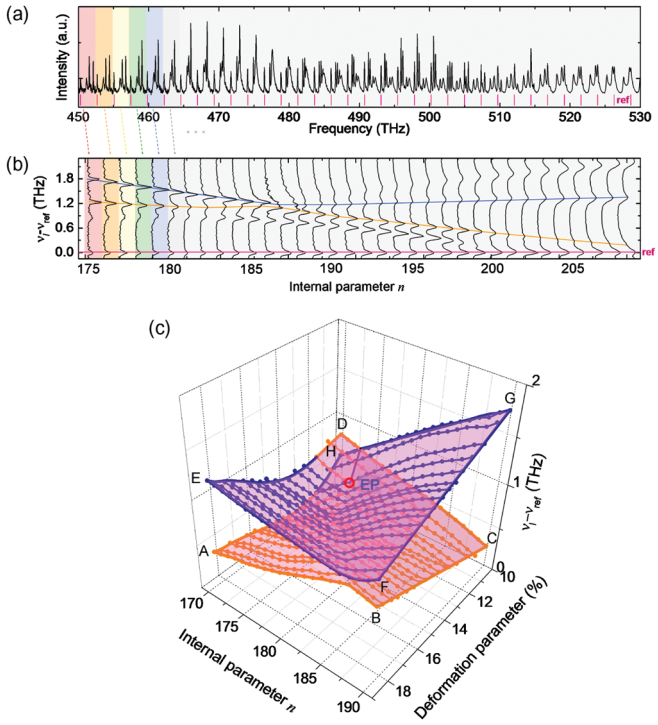

FIG. 4 (color). (a) The observed spectrum for $\eta = 0.187$. (b) The relative frequencies of observed quasieigenmodes with respect to the reference frequency of the same n as a function of n. (c) Eigenfrequency surfaces of two coupled states $l = 2$ (orange dots) and $l = 4$ modes (blue dots) in n-η parameter space show a complex-square-root-like topology with a branch-point singularity at the EP, $(n_0, \eta_0) = (175, 0.125)$.

then evenly divided into segments with each being as wide as one free spectral range of the $l_0 = 3$ WGM so that each segment is indexed as n of that WGM. This n is precisely the internal parameter used throughout this work. The relative frequencies of observed quasieigenmodes assigned with n, with respect to the reference frequency of the same n, are then plotted as a function of n as shown in Fig. 4(b). By repeating this procedure for other η and then combining the results as a function of n and η, we finally obtain the eigenfrequency surfaces $E_{\pm}(n, \eta)$ as shown in Fig. 4(c). The resulting surfaces exhibit a complex-square-root-function-like topology with a branch-point singularity at the EP located approximately at $(n_0, \eta_0) = (175, 0.125)$, where the transition between MC and AMC of $l_0 = 1$ and 4 modes takes place.

The singular topology of the eigenenergy surfaces around the EP result in a fundamental inconsistency in assigning mode labels to quasieigenmodes. In order to illustrate this point, let us consider a cyclic variation of (n, η) as shown in Fig. 4(c): $(170, 0.18) \rightarrow (190, 0.18) \rightarrow (190, 0.10) \rightarrow (170, 0.10) \rightarrow (170, 0.18)$ enclosing the EP. If we choose the $l = 2$ mode at $(170, 0.18)$ and follow the mode under this cyclic variation, we end up with a different $l = 4$ mode in the end after traversing $A \rightarrow B \rightarrow C \rightarrow D \rightarrow E$ on the energy surface. What happens is that the mode label abruptly changes from $l = 2$ to $l = 4$ when we pass by the EP during the adiabatic process of increasing η ($D \rightarrow E$); moreover, there is no way to avoid this inconsistency however differently we label the modes. We have to perform the cyclic variation once more, traversing $E \rightarrow F \rightarrow G \rightarrow H \rightarrow A$ around the EP, in order to come back to the same starting mode. This consideration reveals a fundamental inconsistency in assigning mode labels to quasieigenmodes in nonintegrable open systems. This ambiguity is a direct consequence of the singular topology around the EP.

In conclusion, we have observed an EP or the transition point between MC and AMC in a COM by utilizing different output coupling efficiencies in those two cases. The observed quasieigenfrequencies exhibit a branch-point topology, the very origin of the impossibility of consistent mode labeling in these open chaotic systems. Our spectroscopic method using output coupling efficiency can be applied to other optical and optomechanical systems to resolve MC or AMC static mode envelopes [19].

This work was supported by NRL and WCU grants. S. W. K. was supported by KRF Grant No. 2008-314-C00144. S. Y. L. was supported by the BK21 program.

*kwan@phya.snu.ac.kr

[1] S. M. Spillane *et al.*, Nature (London) **415**, 621 (2002).
[2] A. M. Armani *et al.*, Science **317**, 783 (2007).
[3] A. A. Savchenkov *et al.*, Phys. Rev. Lett. **101**, 093902 (2008).
[4] T. J. Kippenberg and K. J. Vahala, Science **321**, 1172 (2008).
[5] H.-J. Stöckmann, *Quantum Chaos: An Introduction* (Cambridge University Press, Cambridge, 1999).
[6] J. Wiersig and M. Hentschel, Phys. Rev. A **73**, 031802(R) (2006).
[7] J. Wiersig, Phys. Rev. Lett. **97**, 253901 (2006).
[8] W. D. Heiss, Phys. Rev. E **61**, 929 (2000).
[9] M. V. Berry and D. H. J. O'Dell, J. Phys. A **31**, 2093 (1998).
[10] I. Rotter, J. Phys. A **42**, 153001 (2009).
[11] A. L. Shuvalov *et al.*, Acta Mech. **140**, 1 (2000).
[12] M. K. Oberthaler *et al.*, Phys. Rev. Lett. **77**, 4980 (1996).
[13] O. Latinne *et al.*, Phys. Rev. Lett. **74**, 46 (1995).
[14] C. Dembowski *et al.*, Phys. Rev. Lett. **86**, 787 (2001).
[15] C. Dembowski *et al.*, Phys. Rev. Lett. **90**, 034101 (2003).
[16] H. Cartarius *et al.*, Phys. Rev. Lett. **99**, 173003 (2007).
[17] S. Y. Lee *et al.*, Phys. Rev. A **78**, 015805 (2008).
[18] S.-B. Lee *et al.*, Phys. Rev. A **80**, 011802(R) (2009).
[19] T. Carmon *et al.*, Phys. Rev. Lett. **100**, 103905 (2008).
[20] S. Moon *et al.*, Opt. Express **16**, 11 007 (2008).
[21] J. Yang *et al.*, Rev. Sci. Instrum. **77**, 083103 (2006).
[22] S.-B. Lee *et al.*, Phys. Rev. A **75**, 011802(R) (2007).
[23] S.-B. Lee *et al.*, Phys. Rev. Lett. **88**, 033903 (2002).
[24] *Cavity Quantum Electrodynamics*, edited by P. Berman (Academic Press, New York, 1993).
[25] P. Chylek *et al.*, Opt. Lett. **16**, 1723 (1991).